Materials Letters 328 (2022) 133138

Contents lists available at ScienceDirect

Materials Letters

journal homepage: www.elsevier.com/locate/matlet

High performance inorganic filterless narrowband photodetectors

Xinye Fan [a,b], Yiren Chen [a,*], Zhiwei Zhang [a], Guoqing Miao [a], Hong Jiang [a], Hang Song [a,*]

[a] State Key Laboratory of Luminescence and Applications, Changchun Institute of Optics, Fine Mechanics and Physics, Chinese Academy of Sciences, Changchun 130033, China

[b] University of Chinese Academy of Sciences, Beijing 100039, China

ARTICLE INFO

Keywords:
Epitaxial growth
Sensors
Narrowband photodetector
Filterless
Group-III nitride semiconductor

ABSTRACT

The filterless narrowband photodetector is emergent in the field of optoelectric detection due to its spectral discrimination and avoiding interference from other bands. Distinguished from the presently developing strategy based on organic semiconductors, a strategy based on bandpass response behavior by constructing two kinds of group-III nitride semiconductors with different bandgap is proposed. Through functional verification of the prototype device, the results show that high performance filterless narrowband photodetector can be obtained by this strategy. Moreover, the full-width at half maximum and the response band of the bandpass response behavior can be adjusted by manipulating the alloy components.

1. Introduction

The narrowband photodetector with full-width at half maximum (FWHM) of only tens of nanometers can perform spectral discrimination and avoid interference from other bands that are not of interest. It has promising applications in image sensing, chemical analysis, environmental surveillance, and emerging artificial intelligence networks such as augmented/virtual reality, advanced autopilot assistance systems [1–3]. Nowadays, commercially available narrowband photodetectors that can be used for spectral discrimination are realized by integrating external additional optical filters with broadband inorganic semiconductor (mainly silicon-based) photodiodes [4,5]. However, the use of external optical filter not only increases the architectural complexity and the cost of the photodetector, but also limits its detection sensitivity due to additional optical interface scattering and filtering loss [5,6]. Developing filterless narrowband photodetectors is thus proposed as an alternative strategy. So far, filterless narrowband strategy has been mainly implemented in organic semiconductors and organic–inorganic hybrid perovskite materials based on the principles, including: (1) charge collection narrowing (CCN) [7,8], optical field regulation by plasmonic effect [9,10], charge injection narrowing (CIN) [11], exciton dissociation narrowing (EDN) [5], and so on. Considering the application requirements in extreme environments such as high temperature, high pressure and strong radiation, photodetectors developed by full inorganic semiconductors have their distinctive advantages [12]. As a representative of inorganic semiconductor materials, group-III nitride semiconductors not only have stable physical and chemical properties and excellent radiation resistance that qualify for extreme environments, but also have the advantage of realizing intrinsic cutoff at a specified detection wavelength by adjusting the alloy component, making them ideal materials for the development of narrowband photodetectors.

Herein, a full inorganic filterless narrowband photodetector based on group-III nitride semiconductors is fabricated, which presents a narrow FWHM of <50 nm. The narrowband response characteristic is a bandpass response behavior realized by the cooperation of the GaN window layer and the InGaN/GaN multiple quantum wells (MQWs) optical absorption layer. The GaN window layer acts as optical filter allowing the light with a wavelength greater than its intrinsic cutoff wavelength (about 365 nm) to pass through and the InGaN/GaN MQWs optical absorption layer absorbs the light with a wavelength shorter than its intrinsic cutoff wavelength, resulting in the bandpass response behavior. The performances of the narrowband photodetector such as detection band, FWHM can easily meet the requirements of different applications by adjusting the alloy components of the window layer and the optical absorption layer.

2. Experimental procedure

2.1. Material epitaxy

The structural material of the narrowband photodetectors was based

* Corresponding authors.
E-mail addresses: chenyr@ciomp.ac.cn (Y. Chen), songh@ciomp.ac.cn (H. Song).

https://doi.org/10.1016/j.matlet.2022.133138
Received 29 May 2022; Accepted 5 September 2022
Available online 10 September 2022

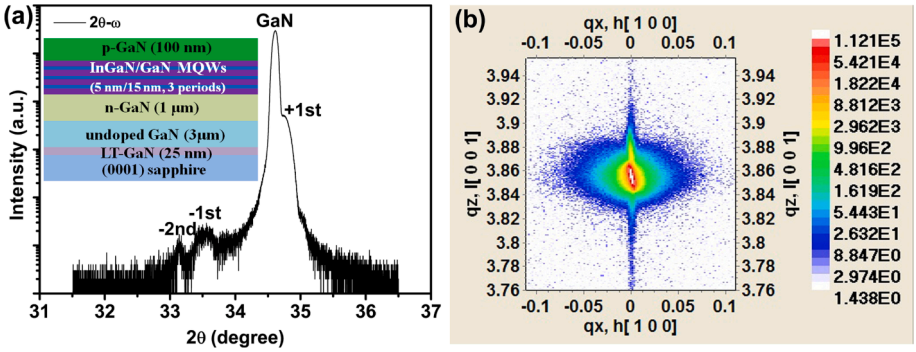

Fig. 1. X-ray diffraction images (a) (0002)-plane 2θ-ω scanning curve of the material and (b) The symmetrical RSM around (0002) plane. The material structure is shown in inset of (a).

on typical InGaN/GaN MQWs light-emitting diode (LED), which was grown on c-plane sapphire substrates by low-pressure metal–organic chemical vapor deposition (MOCVD). In the process, trimethylgallium/triethylgallium (TMGa/TEGa), trimethylindium (TMIn), and ammonia (NH_3) were used as Ga, In, and N precursors, respectively, while silane (SiH_4) and dicyclopentadienyl magnesium (Cp_2Mg) were use as the n- and p-type dopants. The growth process was described as follows: prior to the growth of low-temperature GaN (LT-GaN) buffer layer, the substrate was thermally desorbed at 1050 °C for 10 min under H_2. After a 25-nm thick LT-GaN buffer layer was deposited at 550 °C, the temperature was ramped up to 1020 °C for the deposition of a 3-μm thick unintentional doped GaN and a 1-μm thick Si-doped GaN (*n*-GaN) epilayers in sequence. Then, a periodically modulated TMIn source and growth temperature mode was used to prepare three cycles of 5 nm $In_{0.14}Ga_{0.86}N$/15 nm GaN MQWs. Here, the growth temperatures for GaN barrier and $In_{0.14}Ga_{0.86}N$ well layers were 800 °C and 680 °C, respectively. Finally, a 100-nm thick p-GaN layer was grown on the MQWs layer.

2.2. Device fabrication

Prior to device fabrication, the material was rapidly annealed at 900 °C in an N_2 atmosphere for 60 s to activate the Mg dopants in the p-GaN layer. Then, an 80-μm square mesa was fabricated by standard photolithography and inductively coupled plasma (ICP) etching methods. Subsequently, a Ni/Au (30 nm/200 nm) electrode and a Ti/Al/Ni/Au (30 nm/100 nm/20 nm/200 nm) multi-electrode were deposited on top of and around the mesa by e-beam evaporation in sequence.

2.3. Characterization

A high-resolution X-ray diffractometer (HRXRD, Bruker D8) was used to measure the 2θ-ω scanning curve and the reciprocal space mapping (RSM) image around (0002) plane. The current–voltage (I-V) characteristic of the device was measured by a semiconductor parameter analyzer (Agilent B1500A). The spectral response feature of the device was obtained by an UV/visible spectral response testing system which was equipped with a xenon lamp as the light source and an UV-enhanced Si-based photodetector as the standard calibrated photodetector [13]. The electro-luminescent (EL) spectrum of the device was measured by UV/visible mini-spectrometer (USB2000+, Ocean Optics). A dual beam scanning photometer (UV-3101PC, Shimadzu) was used to measure the transmission and absorption properties of the material. The transient response spectrum of the device was stimulated by a tunable laser (Continuum, Horizon OPO) at 380 nm and recorded by a digital oscilloscope (Tektronix 5104).

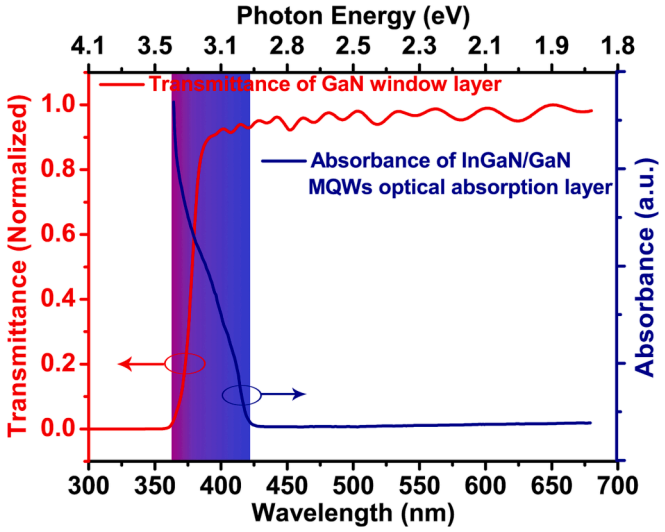

Fig. 2. The transmission spectrum of GaN window layer and the absorption spectrum of $In_{0.14}Ga_{0.86}N$/GaN MQWs optical absorption layer.

3. Results and discussion

The material of the filterless photodetector based on group-III nitride semiconductors is prepared by MOCVD, whose structural diagram is shown in inset of Fig. 1(a). In order to evaluate the crystal quality, the high-resolution X-ray diffraction images of the material are presented in Fig. 1(a) and (b). The (0002)-plane 2θ-ω scanning curve in Fig. 1(a) presents two-level satellite peaks in addition to the main peak of GaN indicating its high quality structural characteristic. A well-resolved main peak with a series of contour lines presented in the RSM around the (0002) reflection (Fig. 1(b)) indicates an excellent lattice arrangement.

Fig. 2 presents the transmission spectrum of GaN window layer and the absorption spectrum of $In_{0.14}Ga_{0.86}N$/GaN MQWs optical absorption layer. Since the bandgap of GaN (E_{gGaN}) is 3.4 eV, the incident photons will be absorbed when their energy ($h\nu$) is equal to or higher than E_{gGaN}. On the contrary, the photons with energy lower than E_{gGaN} will penetrate through. Therefore, the GaN layer acts as a window layer filtering out the incident photons with $h\nu \geq E_{gGaN}$, enabling the photons with energy lower than E_{gGaN} (or wavelength longer than 365 nm) to transmit, as seen in the red line of Fig. 2. Meanwhile, the $In_{0.14}Ga_{0.86}N$/GaN MQWs layer will absorb the transmitted photons with an absorption threshold at about 2.95 eV (or about 420 nm), as demonstrated in the blue line of Fig. 2. In this process, it generates electron-hole pairs, which are separated and transported under the combined action of the built-in electric field and the applied electric field in PN junction to form photocurrent, thus realizing optoelectric detection. That is to say, it acts

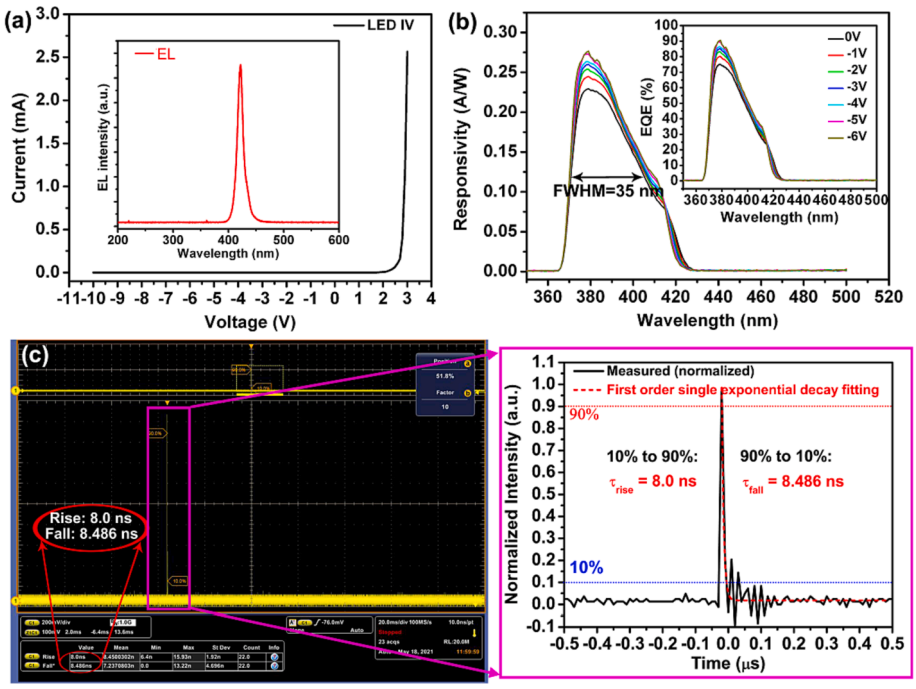

Fig. 3. (a) EL and dark I-V characteristics of the device. (b) The measured spectral responsivities and corresponding EQEs under different applied bias voltages. (c) Transient spectral response of the device.

as the optical absorption layer to achieve photoelectric conversion. The bandpass response behavior is based on the basic principle of constructing two kinds of semiconductors with different bandgap, in which the wide-bandgap semiconductor acts as the light filter layer and the narrow-bandgap one acts as the light absorption layer. Moreover, the width of the bandpass response behavior can be adjusted by controlling both bandgaps.

Having established the basic principle of achieving a filterless narrowband photodetector based on bandpass response behavior, a photodetector using for functional verification is fabricated. Fig. 3(a) presents the typical I-V and EL characteristics of the photodetector. Due to the quantum confinement effect of the $In_{0.14}Ga_{0.86}N$/GaN MQWs layer, its quasi-two-dimensional exciton effect makes the photodetector have a strong absorption peak around 410 nm, as shown in inset of Fig. 3 (a) [14]. In Fig. 3(b), the measured spectral responsivities and corresponding external quantum efficiencies (EQEs) of the photodetector under different applied bias voltages are shown. As can be seen, the response spectra present bandpass response behavior ranging from 365 nm to 425 nm with a peak located at 380 nm and a FWHM of about 35 nm. The peak responsivity and corresponding EQE at zero-bias are measured as 0.229 A/W and 75 % while 0.277 A/W and 90.6 % at 6 V reverse bias. The reason for the slight deviation between absorption spectrum and measured spectrum can be ascribed to the intrinsic spontaneous and piezoelectric polarization effects of nitride material [15]. The transient spectral response of this filterless narrowband photodetector is also presented in Fig. 3(c), which has a 10–90 % rise time of 8.0 ns and a 90–10 % decay time of 8.486 ns under zero-bias, indicating a good response feature.

4. Conclusions

In summary, the strategy of achieving a filterless narrowband photodetector based on bandpass response behavior by constructing two kinds of inorganic semiconductors with different bandgap is proposed in this paper. A filterless narrowband photodetector based on GaN window layer and InGaN/GaN MQWs optical absorption layer is prepared for functional verification. It presents a bandpass response behavior ranging from 365 nm to 425 nm with a FWHM of about 35 nm. The responsivity and EQE are 0.277 A/W and 90.6 % at 6 V reverse bias respectively, which also has a fast transient response as short as 8.486 ns. Following this strategy, the FWHM and the response band of the bandpass response behavior can be adjusted by controlling both bandgaps of window layer and absorption layer.

Declaration of Competing Interest

The authors declare that they have no known competing financial interests or personal relationships that could have appeared to influence the work reported in this paper.

Acknowledgment

This work was partially supported by National Natural Science Foundation of China (Grant No. 61504144), and Department of Science and Technology of Jilin Province (Grant No. 20170520156JH).

References

[1] S.B. Anantharaman, K. Strassel, M. Diethelm, et al., J. Mater. Chem. C 7 (2019) 14639–14650.
[2] Q. Lin, A. Armin, P.L. Burn, P. Meredith, Nat. Photon. 9 (2015) 687–695.
[3] F.P. García de Arquer, A. Armin, P. Meredith, E.H. Sargent, Nat. Rev. Mater. 2 (2017) 16100.
[4] S. Yokogawa, S.P. Burgos, H.A. Atwater, Nano Lett. 12 (2012) 4349–4354.
[5] B. Xie, R. Xie, K. Zhang, et al., Nat. Commun. 11 (2020) 2871.
[6] W. Li, S. Li, L. Duan, et al., Org. Electron. 37 (2016) 346–351.
[7] A. Armin, R.D. Jansen-van Vuuren, N. Kopidakis, et al., Nat. Commun. 6 (2015) 6343.
[8] Y. Fang, Q. Dong, Y. Shao, et al., Nat. Photon. 9 (2015) 679–686.
[9] A. Sobhani, M.W. Knight, Y. Wang, et al., Nat. Commun. 4 (2013) 1643.
[10] X. Tang, G.F. Wu, K.W.C. Lai, J. Mater. Chem. C 5 (2017) 362–369.
[11] M. Liu, J. Wang, Z. Zhao, et al., J. Phys. Chem. Lett. 12 (2021) 2937–2943.
[12] Q. Cai, H. You, H. Guo, et al., Light Sci. Appl. 10 (2021) 94.
[13] Y. Chen, Z. Zhang, G. Miao, et al., Mater. Lett. 281 (2020), 128638.
[14] P. Qi, Y. Luo, B. Shi, et al., eLight 1 (2021) 6.
[15] A. Hangleiter, T. Langer, P. Henning, et al., Proc. SPIE 10104 (2017) 101040Q.